Talanta 83 (2011) 1173–1180

Contents lists available at ScienceDirect

Talanta

journal homepage: www.elsevier.com/locate/talanta

Multivariate curve-resolution analysis of pesticides in water samples from liquid chromatographic–diode array data

Rubén M. Maggio, Patricia C. Damiani, Alejandro C. Olivieri*

Departamento de Química Analítica, Facultad de Ciencias Bioquímicas y Farmacéuticas, Universidad Nacional de Rosario, Instituto de Química de Rosario (IQUIR-CONICET), Suipacha 531, Rosario, S2002LRK, Argentina

ARTICLE INFO

Article history:
Available online 24 July 2010

Keywords:
Chromatographic-spectral matrices
Multivariate curve resolution
Pesticide analysis

ABSTRACT

Liquid chromatographic–diode array detection data recorded for aqueous mixtures of 11 pesticides show the combined presence of strongly coeluting peaks, distortions in the time dimension between experimental runs, and the presence of potential interferents not modeled by the calibration phase in certain test samples. Due to the complexity of these phenomena, data were processed by a second-order multivariate algorithm based on multivariate curve resolution and alternating least-squares, which allows one to successfully model both the spectral and retention time behavior for all sample constituents. This led to the accurate quantitation of all analytes in a set of validation samples: aldicarb sulfoxide, oxamyl, aldicarb sulfone, methomyl, 3-hydroxy-carbofuran, aldicarb, propoxur, carbofuran, carbaryl, 1-naphthol and methiocarb. Limits of detection in the range 0.1–2 $\mu g\,mL^{-1}$ were obtained. Additionally, the second-order advantage for several analytes was achieved in samples containing several uncalibrated interferences. The limits of detection for all analytes were decreased by solid phase pre-concentration to values compatible to those officially recommended, i.e., in the order of 5 $ng\,mL^{-1}$.

1. Introduction

Collection of multi-dimensional chromatographic information, and data processing by advanced chemometric algorithms constitute a fruitful combination of techniques, recently applied to diverse research areas, such as analyte quantitation [1–7], sample classification [8] and metabolomics studies [9]. Chemometrics is required whenever perfect separation of the various sample components cannot be achieved by the employed chromatographic system, leading to unwanted overlapping peaks in the retention time dimension. The situation has been termed the 'cocktail party effect' [10]. In these cases, selectivity may be mathematically restored by applying multivariate data analysis [11]. In particular, the so-called second-order advantage can be achieved, a property which is inherent to matrix instrumental data, and implies that analytes can be quantitated in samples containing potential interferences [11]. Examples from the recent literature on quantitations aided by the second-order advantage are the determination of pesticides in wine [12] and river and wastewater samples [13], fluoroquinolone antibiotics in urine [14], and sulfonates [15] and polycyclic aromatic hydrocarbons in water [7]. In all of these cases, signals arising from coeluting analytes or foreign components were modeled by powerful second-order multivariate algorithms.

For the convenient processing of second-order data achieving the second-order advantage, analyst have only certain algorithms available [1,2,16]. The latter may be classified as (1) alternating least-squares (ALS) models, such as multivariate curve resolution–alternating least-squares (MCR–ALS) [17] and parallel factor analysis (PARAFAC) [18], some of its variants including PARAFAC2 [19–21], (2) direct least-squares models, such as bilinear least-squares (BLLS) in its several versions [22–24], (3) latent structured models, such as unfolded partial least-squares (U-PLS) [25], where 'unfolded' refers to working with previously vectorized data matrices [26], and multi-way PLS (N-PLS) [27], both combined with residual bilinearization (RBL) [28–31], and (4) eigenvector–eigenvalue models, such as the generalized rank annihilation method (GRAM) [32].

It should be noticed that some of the above chemometric methods are restricted to work with trilinear data, which basically require that each chemical component shows a unique profile in all samples, in both the spectral and temporal dimensions. In liquid chromatographic runs, retention time shifts usually occur from sample to sample, destroying the data trilinearity. In these cases, a useful alternative is to analyze the data with more flexible algorithms, which allow a given component to present different time profiles in different samples, such as PARAFAC2 or MCR–ALS [7]. Latent structured methods such as U-PLS/RBL and N-PLS/RBL are in principle able to deal with trilinearity losses. However, experience

* Corresponding author. Tel.: +54 341 4372704; fax: +54 341 4372704.
E-mail addresses: olivieri@iquir-conicet.gov.ar, aolivier@fbioyf.unr.edu.ar (A.C. Olivieri).

0039-9140/$ – see front matter © 2010 Elsevier B.V. All rights reserved.
doi:10.1016/j.talanta.2010.06.059

indicates that this success cannot be achieved with a limited number of calibration samples, probably requiring a sufficiently large and representative training set of samples [14].

Another option for data processing of chromatographic-spectral data is to mathematically restore the lost trilinearity, so that the analyte peaks are properly aligned. Several methods are available to perform such alignment, with two basic philosophies: (1) to take advantage of the matrix data structure, such as rank alignment [33,34], iterative target transformation factor analysis (ITTFA) [13], and a recently discussed suitably initialized and constrained PARAFAC alignment [35] and (2) to seek maximum correlation between chromatograms, such as in the so-called ChromAlign algorithm [36] and also in single and multi-wavelength correlation optimized warping (COW) [37–40]. However, this activity is not successful, in principle, in the presence of potential interferences in unknown samples, with the exception of ITTFA [13] and PARAFAC alignment [35]. These two latter techniques are able to accommodate for coeluting interferents not modeled in the calibration phase; however, they cannot deal with retention time shifts which are not constant. A general alignment method, which would correct both for interferents and varying time shifts has yet to be developed. In the meantime, alternative philosophies based on MCR–ALS or PARAFAC2 data processing may be useful for solving the analytical presently discussed problem. Recent work from our laboratory indicated better performance with the former model in the case of multi-analyte quantitation in the presence of uncalibrated interferences, mainly because of the possibility of building a more constrained model in MCR–ALS in comparison with PARAFAC2 [7].

In the present report, we selected MCR–ALS as the algorithm of choice for processing data from high performance liquid chromatography (HPLC) with diode array detection. We discuss its behavior towards the quantitation of the following 11 pesticides in water samples: aldicarb sulfoxide (ALDSX), oxamyl (OXA), aldicarb sulfone (ALDSN), methomyl (MET), 3-hydroxy-carbofuran (3HOC), aldicarb (ALD), propoxur (PRO), carbofuran (CBF), carbaryl (CBR), α-naphthol (NAP) and methiocarb (MTC). The presence of carbamates and their degradation products in surface and drinking waters is potentially harmful for humans due to their proven toxicity. This is the cause of the continued interest in the development of analytical methods for monitoring this family of compounds. The above-mentioned pesticides have been determined in validation samples which do only contain mixtures of the analytes, and also in additional test samples, containing potential interferents not included in the calibration set. These potential interferents, α-naphthyl acetic acid (ANA) and 2-methyl-4-chlorophenoxyacetic (MPCA) are a plant growth regulator and a phenoxy herbicide respectively, which may also be present in water samples because they are widely used for agricultural purposes. The interfering test samples are intended to mimic truly unknown samples composed of uncalibrated substances, where an unknown background may occur. The inclusion of known chemical components in these test samples had the purpose of checking whether the multivariate algorithm was able to successfully retrieve their corresponding spectral and retention time profiles.

A previous chromatographic analysis of the presently studied compounds accomplished full resolution using ternary solvent gradient elution, and requiring approximately 35 min [41]. In comparison, under the presently discussed isocratic conditions, the same compounds in the same type of mixtures eluted in less than 15 min. Thus, a drastic reduction in elution time and consequently in solvent consumption was achieved when the isocratic mode was used. However, overlapping of the analyte retention times is observed in this case, requiring chemometric techniques such as MCR–ALS to complement bidimensional chromatographic-spectral data.

2. Theory

2.1. MCR–ALS

Multivariate curve-resolution coupled to alternating least-squares is capable of handling data matrices with varying component profiles in one of the data dimensions. This makes it especially suitable for the convenient processing of liquid chromatographic–diode array detection (LC–DAD) matrix data discussed in the present paper.

In MCR–ALS, an augmented data matrix is created from a group of data matrices for several samples. We consider matrices of size $J \times K$, where J is the number of data points in the spectral dimension and K the number of data points in the temporal dimension (in the present case, this is the dimension where profiles may change from sample to sample). In general, augmentation can be performed in either direction, depending on the type of experiment being analyzed. In the present case, however, the mode of augmentation should be the temporal one. Therefore, the bilinear decomposition of the augmented matrix is performed according to the expression:

$$\mathbf{D} = \mathbf{C}\mathbf{S}^{\mathrm{T}} + \mathbf{E} \tag{1}$$

where the rows of **D** contain the spectra measured for different samples at several values of the temporal dimension, the columns of **C** contain the profiles of the intervening species in the temporal dimension, the columns of **S** their related spectra, and **E** is a matrix of residuals not fitted by the model. The sizes of these matrices are **D**, $JI \times K$, **C**, $JI \times N$, **S**, $K \times N$, **E**, $JI \times K$ (N is the number of responsive components). As can be seen, **D** contains data for the I different samples.

The iterative ALS procedure aims at minimizing the Frobenius norm of **E**, and is initialized using an initial estimation of the spectral or concentration profiles for each intervening species. Different methods are used for this purpose, such as evolving factor analysis (EFA) [42] if the initial time profiles are sought, or the determination of the purest variables (PURE) [43–45] when the initial spectra are required. Known spectra for the contributing components can also be employed for initialization. If the initial estimations are the spectral profiles, the unconstrained least-squares solution for the concentration profiles can be calculated from the expression:

$$\mathbf{C} = \mathbf{D}(\mathbf{S}^{\mathrm{T}})^{+} \tag{2}$$

where $(\mathbf{S}^{\mathrm{T}})^{+}$ is the pseudoinverse of the spectral matrix $\mathbf{S}^{\mathrm{T}}$, which is equal to $[\mathbf{S}(\mathbf{S}^{\mathrm{T}}\mathbf{S})^{-1}]$ when $\mathbf{S}^{\mathrm{T}}$ is full rank [46]. If the initial estimations were the concentration profiles, the unconstrained least-squares solution for the spectra can be calculated from the expression:

$$\mathbf{S}^{\mathrm{T}} = \mathbf{C}^{+}\mathbf{D} \tag{3}$$

where $\mathbf{C}^{+}$ is the pseudoinverse of **C** [$\mathbf{C}^{+} = (\mathbf{C}^{\mathrm{T}}\mathbf{C})^{-1}\mathbf{C}^{\mathrm{T}}$], when **C** is full rank [46]. Both steps can be implemented in an alternating least-squares cycle, so that in each iteration new **C** and $\mathbf{S}^{\mathrm{T}}$ matrices are obtained.

During the iterative recalculations of **C** and $\mathbf{S}^{\mathrm{T}}$, a series of constraints are applied to improve these solutions, to give them a physical meaning, and to limit their possible number for the same data fitting [47]. Iterations continue until an optimal solution is obtained that fulfils the postulated constraints and the established convergence criteria. For example, non-negativity constraints are applied to the concentration profiles, due to the fact that the concentrations of the chemical species are always positive values or zero. Non-negativity constraints are also applied for spectra such as UV–visible. Unimodality is a constraint which can be applied to profiles having a single maximum, as in the case of chromatographic profiles. In the case of the test samples containing uncalibrated interferents, a useful additional restriction is to so-called

correspondence among species and samples. The latter one provides information as to the presence or absence of each analyte in each sample (for example, uncalibrated interferents are present in the unknown samples, but absent in the calibration samples). Finally, closure constraints may be applied for the fulfilment of chemical mass balance equations among different chemical species in equilibrium or in kinetics (not applicable to the presently discussed data).

After MCR–ALS decomposition of **D**, concentration information contained in **C** can be used for quantitative predictions, by first defining the analyte concentration score as the area under the profile for the *i*th sample:

$$a(i,n) = \sum_{j=1+(i-1)J}^{iJ} C(j,n) \quad (4)$$

where $a(i,n)$ is the score for the component n in the sample i. Calibration samples are always within those employed to build the augmented matrix **D**. Their associated scores can be used to build a pseudo-univariate calibration graph against the nominal analyte concentrations. Prediction of analyte concentration in unknowns then proceeds by interpolation of the corresponding analyte scores in the calibration graph.

2.2. Software

All calculations were made using MATLAB 7.0 [48]. MCR–ALS was implemented using the graphical interface provided by Tauler in his web page http://www.ub.edu/mcr/welcome.html [49]. A short MATLAB routine was written to convert scores from Eq. (4) to predicted concentrations by building the pseudo-univariate calibration curve and interpolation of the test scores. All programs were run on an IBM-compatible microcomputer with an Intel core duo T7100, 1.80 GHz microprocessor and 2.00 Gb of RAM.

3. Experimental

3.1. Reagents and solutions

All experiments were performed with ALDSX, OXA, ALDSN, MET, 3HOC, ALD, PRO, CBF, CBR, NAP, MTC, ANA and MPCA purchased from Aldrich Chemical Co. (Milwaukee, Wisconsin, USA) and used as received. HPLC-grade acetonitrile and double distilled water were employed for analyses. Solvents were filtered through 0.47 μm nylon filters.

All solutions were prepared in standard volumetric flasks. Stock standard solutions of ALDSX (2.500 mg mL^{-1}), OXA (1.570 mg mL^{-1}), ALDSN (1.180 mg mL^{-1}), MET (1.100 mg mL^{-1}), 3OHC (0.860 mg mL^{-1}), ALD (1.210 mg mL^{-1}), PRO (1.150 mg mL^{-1}), CBF (0.990 mg mL^{-1}), CBR (1.270 mg mL^{-1}), NAP (1.120 mg mL^{-1}), MTC (0.770 mg mL^{-1}), ANA (0.800 mg mL^{-1}) and MPCA (4.000 mg mL^{-1}) were prepared in acetonitrile and stored at 4 °C until used.

3.2. Apparatus

Chromatographic runs were performed on an HP 1100 liquid chromatograph (Agilent Technologies, Waldbronn, Germany) consisting of a quaternary pump, a manual injector fitted with a 20 μL loop and a diode array UV–visible detector set at a wavelength range from 190 to 300 nm. A C18 column of 150 mm × 4.6 mm, 5 μm particle size was employed (Agilent Sorbax SB). The data were collected using the software HP ChemStation for LC Rev. A.OS.02 [273] HP 1990–1997.

3.3. HPLC procedure

The mobile phase used for all chromatographic runs was a 60:40 (v/v) mixture of water and acetonitrile, delivered at a flow rate of 1.0 mL min^{-1} with a chromatographic system operating under isocratic mode. Each chromatogram was accomplished in ca. 15 min.

3.4. Calibration, validation and test samples

Calibration and validation samples were prepared by measuring appropriate aliquots of the standard solutions, placing them in 10.00 mL volumetric flasks to obtain the desired concentrations, and completing to the mark with acetonitrile.

In order to design the calibration set, preliminary experiments were performed with the pure analytes, showing that the full retention time range could be divided into three relevant regions: a heavily overlapped zone where four analytes appear (ALDSX, OXA, ALDSN, MET and 3OHC), a region of comparatively lower overlapping among three analytes (ALD, PRO and CBF), and a region where the remaining three analytes are fully resolved (CBR, NAP and MTC). Therefore, a calibration set of twelve samples was prepared for building the multivariate models. Nine of these samples corresponded to the concentrations provided by a fractional factorial design at three levels for the four analytes appearing in the first region (i.e., $3^{5-3} = 9$ samples): ALDSX, OXA, ALDSN, MET and 3OHC. Each of the nine samples of the latter design was randomly combined with concentrations for an additional nine-sample set containing ALD, PRO and CBF from a three-level fractional factorial design (i.e., $3^{3-1} = 9$ samples). The remaining 3 samples of the 12-sample set corresponded to blank solutions for the latter eight analytes, and contained CBR, NAP and MTC at three equally spaced concentration levels. For establishing the calibration concentration ranges, the linear range for all components was studied by analyzing six solutions covering the interval 0–20 μg mL^{-1}. It was found that a suitable calibration concentration range was 0.00–12.00 μg mL^{-1} for all analytes. Thus, the 11 analytes were tested by the multivariate model at triplicates of the following 4 concentration levels: 0.00, 3.00, 8.00 and 12.00 μg mL^{-1}.

A validation set of 10 samples was also prepared, containing all 11 analytes in concentrations different than those used for calibration, and following a random design, i.e., the specific concentrations were taken as random numbers generated within the calibration domain.

The potential interferents ANA and MPCA, intended to mimic the occurrence of truly unknown samples with a complex responsive background, have spectra and chromatographic bands which significantly overlap with some of the studied analytes. Therefore, with the purpose of evaluating the proposed strategy in the presence of these 2 interferences, 9 additional test samples were prepared, containing random concentrations of the 11 studied analytes and either one or both interferences, at concentrations of 10.00 μg mL^{-1}. This test set of samples served to explore the achievement of the second-order advantage by the second-order multivariate procedure.

Finally, four real water samples were spiked with some of the analytes at random concentrations, and were subjected to pre-concentration and chromatographic analysis followed by chemometric resolution, in order to test the analytical performance of the presently described methodology in a practical situation.

3.5. Solid phase extraction procedure

Cartridges containing 1 g of a silica gel-C18 solid phase were used to pre-concentrate all analytes from a given sample. The cartridges were conditioned with 2 mL of acetonitrile and 2 mL of doubly distilled water before use. The corresponding volume

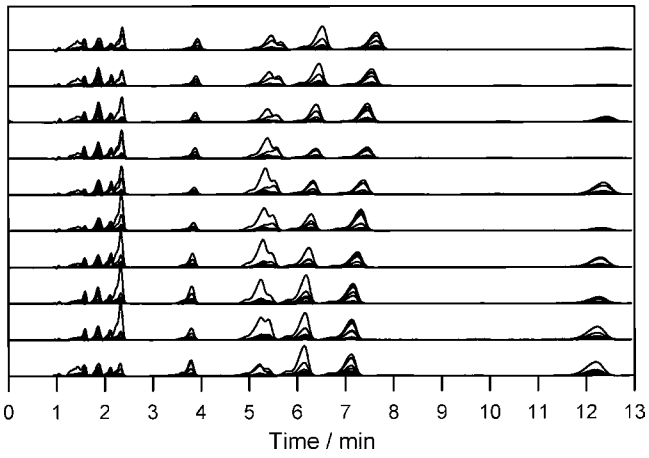

Fig. 1. Liquid chromatograms with diode array detection for the set of validation samples, which contain random concentrations of the 10 studied analytes. Selected spectral traces are superimposed in each chromatographic run. Warping is apparent in the least retained peaks (i.e., retention time from 4.5 to 13 min).

of sample (100 mL) was transferred into a solid phase extraction (SPE) cartridge at a flow rate of 5–7 mL min^{-1}. Cartridges with the absorbed compound were washed with 2 mL distilled water. The compounds were then eluted with 3 mL of acetonitrile under low vacuum using a water pump. The resulting solution was evaporated to dryness in vacuum, the evaporated residue was dissolved in 1 mL of acetonitrile, and finally 20 μL of the resulting solution were injected into the chromatograph for analysis. In this way, a concentration factor of 1:100 was achieved.

4. Results and discussion

4.1. Analysis of the calibration set

Using pure analyte standards, a chromatographic method allowing their partial separation was rationally developed, making proper selection of the range of detected wavelengths and the composition of the mobile phase, in order to obtain an overall chromatographic time of less than 15 min. Under these conditions, when calibration samples were eluted, two clusters of coeluting peaks and several individual, fully resolved peaks appeared in all chromatographic runs (Fig. 1).

Notice in Fig. 1 the warping effect suffered by the chromatograms: the analyte retention times not only shift from run to run, but the magnitude of the shift increases with increasing retention times. This warping effect, combined with the presence of potential interferents in some of the analyzed samples, makes it impossible to align the chromatograms in the time dimension, in order to restore the trilinearity required by most second-order multivariate algorithms. This is the main reason for employing the MCR–ALS algorithm for data processing. Specifically, the latter algorithm was used to process LC–DAD sub-matrices taken at specific retention time ranges. For reasons to be explained below, each chromatographic data matrix was divided in the following time regions: region I (0.6–3.1 min), region II (3.1–4.4 min), region III (4.2–8.3 min), and region IV (11.0–13.0 min) respectively. The spectral absorption range was 190–300 nm for all analytes (Fig. 1).

For each time region, MCR–ALS was first applied to augmented matrices in the time direction, corresponding to the simultaneous analysis of LC–DAD data matrices for the calibration set of samples. In this analysis, initialization of the multivariate algorithm was performed using either previously known pure species spectra from individual analysis of standards, or spectral estimates obtained from the PURE algorithm. Both of the latter alternatives

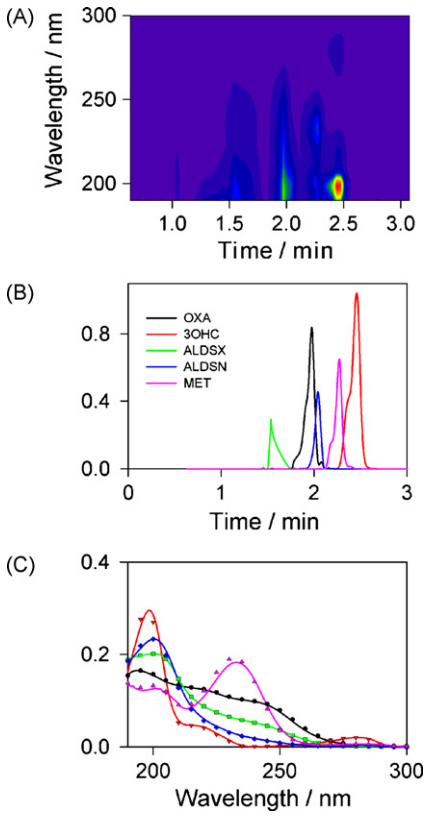

Fig. 2. Results for the analysis of the calibration set of samples. (A) Contour plot around the first cluster peak (region I) containing the analytes ALDSX, OXA, ALDSN, MET and 3OHC for a typical calibration sample. (B) MCR–ALS resolved elution profiles for the same sample, with all analytes indicated. (C) Spectral profiles retrieved by MCR–ALS analysis, which are common to all samples (analyte colors are as in plot B). Superimposed to these profiles are the spectra of pure standards, using symbols with the corresponding analyte colors. The vertical scale in plots (B) and (C) is in arbitrary units.

rendered equally acceptable results. Non-negativity and unimodality were applied during the ALS optimization phase. The resolution of calibration samples provided the characteristic chromatographic profiles and pure spectra for the different analytes. The resolved spectral profiles after MCR–ALS optimization were stored for future use as initial spectral profiles for the analysis of both the validation and test set of samples. After MCR–ALS resolution of the augmented calibration matrix, a pseudo-univariate calibration was carried out for each compound, linearly regressing the scores from Eq. (4) vs. the corresponding nominal concentrations. This was done in order to estimate the corresponding figures of merit, as reported, for example, in Ref. [50].

Five different independent contributions were resolved by MCR–ALS in the first peak cluster corresponding to region I (Fig. 2A). For a typical sample, the five MCR–ALS resolved elution profiles and shown in Fig. 2B, and the spectra (common to alls samples) in Fig. 2C. These five contributions were identified as the analytes ALDSX, OXA, ALDSN, MET and 3OHC, in the latter case by comparison of the MCR-obtained spectra with the actual spectra of the pure compounds (also shown in Fig. 2C using symbols with the same analyte colors). Coelutions shown in Fig. 2A are untreatable by traditional chromatography. However, mathematical resolution using MCR–ALS was still possible by processing second-order LC–DAD data.

Region II contained a fully resolved peak at 3.8 min belonging to ALD. Therefore, the analysis of ALD was done by applying MCR–ALS to the sub-matrix containing its isolated peak. Although this could

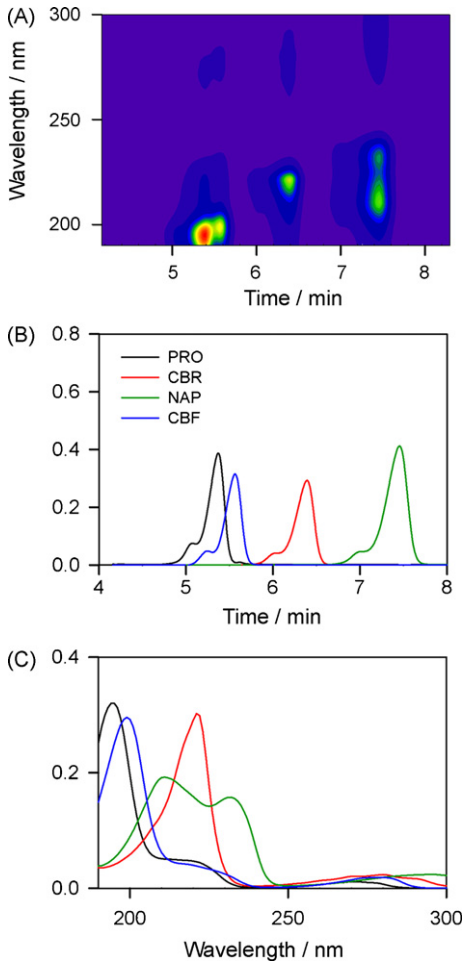

Fig. 3. Results for the analysis of the calibration set of samples. (A) Contour plot around the second cluster peak (region III) containing the analytes ALD, PRO, CBF and CBR for a typical calibration sample. (B) MCR–ALS resolved elution profiles for the same sample, with all analytes indicated. (C) Spectral profiles retrieved by MCR–ALS analysis, which are common to all samples (analyte colors are as in plot B). The vertical scale in plots (B) and (C) is in arbitrary units.

also be done using a univariate strategy, we preferred to determine this analyte using MCR–ALS for consistency.

Region III corresponds to the partially overlapped peaks for PRO and CBF, and also to the isolated peaks for CRB and NAP (Fig. 3A). In the analysis of this region, the contribution from CBF was especially difficult to distinguish from PRO because their absorption spectra are very similar. It should also be noticed that CRB and NAP had to be analyzed together with PRO and CBF. The chromatographic peaks for CRB and NAP are fully resolved in individual chromatograms, but they are partially superimposed with those of PRO and CBF in different chromatograms, due to retention time shifts occurring between different runs (Fig. 1). Once the sub-matrix for region III was resolved by MCR–ALS analysis, time profiles were retrieved (see Fig. 3B for a typical sample) and individual analyte contributions were identified by comparation of the MCR-obtained spectral profiles with those for the pure compounds (Fig. 3C).

Finally, in region IV, the analyte MET did not coelute with any other analyte, and was analyzed as ALD above.

Table 1 shows a summary of the results for all the analyte calibration curves. Good linear relationships between MCR–ALS scores and nominal concentrations were found in all cases. The limits of detection (LOD) were computed as three times the standard deviation for the predicted concentration of the triplicate blank samples with each pseudo-univariate calibration curve. They are

Table 1
Summary of the results from the pseudo-univariate calibration curves for all analytes.[a].

Analyte	Slope (SD)[b]	Intercept (SD)[b]	R^2	$s_{y/x}$	SEN	LOD
ALDSX	0.075 (0.007)	0.09 (0.05)	0.9555	0.08	0.08	2.3
OXA	0.32 (0.01)	0.02 (0.10)	0.9912	0.16	0.32	0.1
ALDSN	0.27 (0.01)	0.29 (0.08)	0.9914	0.14	0.27	1.1
MET	0.46 (0.02)	−0.2 (0.2)	0.9845	0.31	0.46	0.2
3HOC	0.36 (0.01)	0.06 (0.09)	0.9924	0.16	0.37	0.1
ALD	0.125 (0.005)	0.18 (0.04)	0.9869	0.07	0.13	0.2
PRO	0.39 (0.01)	0.20 (0.08)	0.9944	0.15	0.38	0.3
CBF	0.338 (0.008)	0.06 (0.07)	0.9962	0.11	0.34	0.1
CBR	0.624 (0.009)	0.02 (0.05)	0.9987	0.11	0.62	0.1
NAP	1.53 (0.03)	−0.03 (0.11)	0.9988	0.20	0.65	0.2
MTC	1.249 (0.008)	0.05 (0.05)	0.9985	0.11	0.64	0.1

[a] R^2, squared correlation coefficient; $s_{y/x}$, standard deviation of regression residuals; SEN, sensitivity in AU mL μg^{-1}; LOD, limit of detection in μg mL^{-1}.
[b] Standard deviation in parenthesis.

in the order of 0.1–0.3 μg mL^{-1} for most analytes, and 1–2 μg mL^{-1} for ALDSX and ALDSN, meaning that pre-concentration by a factor of 1:100 is required to attain the officially recommended LOD values for the most demanding analyte (PRO).

4.2. Solid phase pre-concentration

Official regulating agencies recommend limits of detection for the presently studied pesticides which are in the range 3–700 ng mL^{-1} for drinking waters [51,52]. The extreme values correspond to PRO (lower limit) and CBR (higher limit). With the aim of reaching limits of detection (LOD) similar to those recommended by regulating agencies, a solid phase extraction procedure was developed for the present analytes (see Section 3.5). The purpose of this procedure was to achieve an LOD value for all analytes around the lowest of the officially recommended values, i.e., ca. 3 ng mL^{-1}. Since the analysis of the figures of merit discussed above for the calibration pseudo-univariate regressions indicated LOD values in the range 0.1–0.3 μg mL^{-1}, the required degree of concentration was 1:100 for the worst possible scenario (analyte PRO). This concentration factor was obtained with the procedure discussed in Section 3.5. The study of individual analytes at a concentration level of 8.00 μg mL^{-1} showed recoveries in the range 87–113%.

4.3. Analysis of the validation set

As indicated above, data matrices were analyzed by creating augmented matrices with sub-matrices corresponding to specific time windows (regions I, II, III and IV). For quantitating the analytes in the validation set of samples, each validation chromatographic LC–DAD data matrix was divided into the selected four time regions. For each time region and for each validation sample, a time-dimension augmented matrix was created. Each augmented matrix contained, adjacent to each other, the sub-matrices corresponding to the calibration samples and to a given validation sample. As before, non-negativity and unimodality constraints were applied during ALS optimization. The MCR–ALS algorithm was initialized using the finally retrieved spectral profiles from the analysis of the calibration set (see previous section). The process was repeated for all validation samples and for all time regions.

After optimization with the multivariate algorithm, the scores corresponding to each analyte in each validation sample were isolated, and prediction proceeded by interpolation into the pseudo-univariate score-concentration calibration plot.

The statistical results when MCR–ALS was applied in this manner are shown in Table 2. As can be observed, the predictions for the eleven analytes are in good agreement with the corresponding nominal values. The relative errors of prediction (REP), computed with respect to the mean calibration concentration of each analyte,

Table 2
MCR–ALS statistical results for the prediction of the studied analytes in the validation set of samples.

Analyte	Recovery[a] (SD) (%)	RMSE[b] ($\mu g\,mL^{-1}$)	REP[b] (%)
ALDSX	100 (17)	1.10	16
OXA	98 (8)	0.67	11
ALDSN	101 (15)	1.00	19
MET	100 (8)	1.12	21
3HOC	101 (5)	0.30	4.4
ALD	100 (11)	1.23	15
PRO	98 (9)	0.63	9.7
CBF	97 (7)	0.38	7.6
CBR	98 (7)	0.53	7.4
NAP	100 (4)	0.26	4.3
MTC	98 (5)	0.40	5.9

[a] Mean recovery for the 10-sample set (standard deviation in parenthesis).
[b] RMSE, root mean square error; REP, relative error of prediction.

are also quoted in Table 2. In view of the complexity of the studied samples, they are reasonable for all analytes, with the largest errors estimated for ALDSX and ALDSN, which showed the worst LOD values (see above), probably due to lower intrinsic sensitivity and/or heavy profile overlap for these two analytes. Further insight into the accuracy of the proposed method can be gathered from the consideration of the elliptical joint confidence region (EJCR) for the slope and intercept of the regression of found vs. nominal concentrations [53]. The conclusion was that all the analyte ellipses (at 95% confidence level) included the theoretically expected point of unit slope and zero intercept, indicating analytical accuracy.

4.4. Analysis of the test set with interferents

The validated LC–DAD/MCR–ALS method was used for the simultaneous determination of some of the studied analytes in the presence of two pesticides (MPCA and ANA) as potential interferents. This final study was carried out in order to test the ability of the methodology in exploiting the second-order advantage which is inherent to second-order data. The samples of the test set contain the sum of the contribution of two foreign constituents, i.e., substances not modelled in the calibration set, and intend to check the algorithm performance towards a sample with an unknown background. The fact that we know the chemical identity of these interferents is a further proof of the modelling power of MCR–ALS, because the finally retrieved spectral and retention time profiles for the interferents can be compared with those known for the pure interferents.

The interferents MPCA and ANA were selected because they coelute with analytes of regions I and II, and display a high degree of spectral overlapping (Figs. 4B, C and 5B, C). Nine samples containing 10.0 $\mu g\,mL^{-1}$ of either MPCA, ANA or both of them simultaneously, and random concentrations of all analytes, were analyzed by LC–DAD/MCR–ALS. Data processing was then carried out in the relevant regions I and II in the same way as explained above for the validation samples, in terms of augmented matrix building and constraints imposed during the ALS algorithmic phase. The correspondence constraint could also be applied in this case, although the results were identical to those obtained without this restriction. Regarding the initial spectra for the interferents, it should be noted that in a general case they are not known *a priori*. Therefore, for each of the test samples, analysis using the PURE methodology was performed, rendering approximations to all pure spectra. Those which differ from the known analyte profiles were then joined with the ones previously employed for the analytes in the validation samples in order to set initial estimations to the spectra.

In region I, seven independent contributions were resolved by MCR–ALS. In Fig. 4B, the retrieved elution profiles of these seven species are shown for one of the investigated test samples. Five of them were identified as the analytes ALDSX, OXA, ALDSN, MET and 3OHC (see spectra in Fig. 4C). Their spectra match those known for the pure analytes and also those retrieved for the validation samples, except for the case of ALDSN, due to extensive spectral overlap in these complex samples. Additional contributions were assigned to the interferent MPCA, causing the presence of two peaks (MPCA1 and MPCA2, one of them is presumably a degradation product of the interferent MPCA). This shows the power of the MCR–ALS algorithm in resolving the individual contributions of the analytes and inteferents, achieving the second-order advantage for quantitative purposes. Additionally, the algorithm may help in the identification of coeluting components, by isolating their spectral and time profiles to be compared with those of potential interferents (Fig. 4B and C).

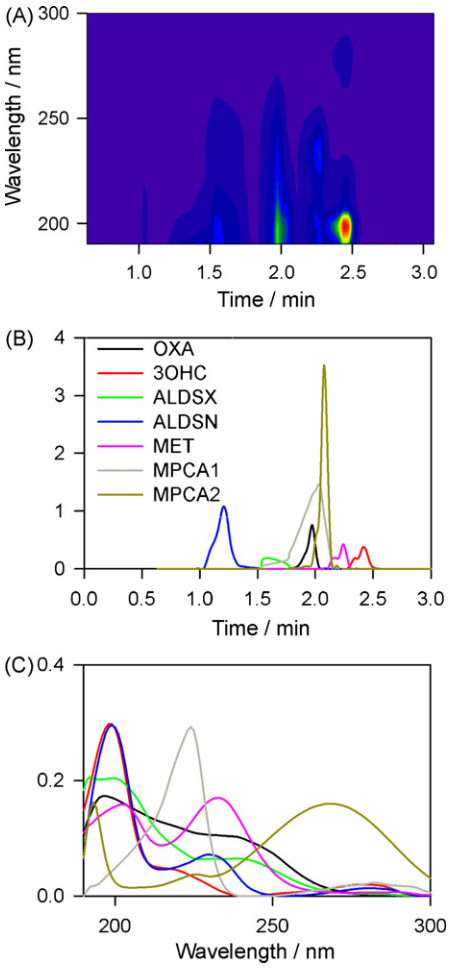

Fig. 4. Results for the analysis of a test sample containing potential interferents. (A) Contour plot around region I containing the analytes ALDSX, OXA, ALDSN, MET and 3OHC and the interferents in a typical test sample. (B) MCR–ALS resolved elution profiles for the same sample, with analytes and interferents indicated. (C) Spectral profiles retrieved by MCR–ALS analysis (analyte colors are as in plot B). The vertical scale in plots (B) and (C) is in arbitrary units.

On the other hand, in region II the ALD peak eluted at ca. 3.8 min, together with an additional peak corresponding to the interferent ANA (Fig. 5A). Thus, ALD was determined by MCR–ALS analysis with the aim of resolving these two components. The result from the MCR–ALS resolution of the augmented matrix (Fig. 5B and C) shows that the peaks were overlapped in both the spectral and retention time dimension.

Table 3 collects the figures of merit for the quantitation in the test set of samples. It is interesting to note that the presence of interferences does not significantly modify the recovery for OXA,

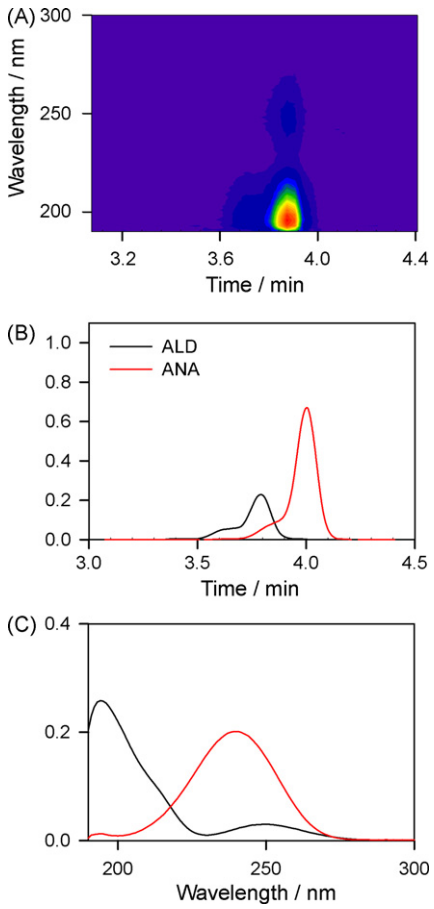

Fig. 5. Results for the analysis of a test sample containing potential interferents. (A) Contour plot around region II containing the analyte ALD and the interferent ANA in a typical test sample. (B) MCR–ALS resolved elution profiles for the same sample, with analytes and interferents indicated. (C) Spectral profiles retrieved by MCR–ALS analysis (analyte colors are as in plot B). The vertical scale in plots (B) and (C) is in arbitrary units.

MET, 3HOC and ALD, which are all reasonable for samples of the complexity of those presently analyzed. The results for ALDSX are comparably more dispersed, causing unsatisfactory REP values and EJCR accuracy results. Finally, poor analytical results were retrieved for ALDSN, possibly due to the large overlapping occurring in both the spectral and retention time dimensions among ALDSN and the pair MPCA1/MPCA2, and to the comparatively larger absorbance of the interferents with respect to the analyte in question. The poor results for ALDSN could also be attributed, in principle, to significant time shifts occurring in the chromatographic maxima for ALDSN when comparing calibration and test samples (see Figs. 2B and 4B), However, this should not constitute a serious problem for the MCR–ALS resolution phase, since this algorithm is able to take into account such temporal shifts within chromatographic runs.

Table 3
MCR–ALS statistical results for the prediction of selected analytes in the test set of samples containing uncalibrated interferents, and in the set of spiked real water samples.

Analyte	Recovery[a] (SD) (%)	RMSE[b] ($\mu g\,mL^{-1}$)	REP[b] (%)
Test set containing interferents			
ALDSX	96 (33)	2.36	32
OXA	110 (23)	1.72	21
MET	111 (19)	1.95	24
3HOC	104 (19)	1.21	16
ALD	89 (8)	0.94	13
Spiked real water samples			
ALDSX	138		
ALDSN	109		
OXA	80		
MET	99		
3HOC	97		
ALD	91		

[a] Mean recovery for the nine-sample set (standard deviation in parenthesis).
[b] RMSE, root mean square error; REP, relative error of prediction.

4.5. Analysis of spiked real water samples

Four real water samples taken from a local river were spiked with the most challenging analytes ALDSX, ALDSN, OXA, MET, 3OHC and ALD, and were subjected to the analytical protocol discussed above. The recovery results are collected in Table 3; they are satisfactory in view of the sample composition. Although the analysis of these samples revealed no significant interference from foreign species, the success in processing the synthetic test set having potential interferences provides confidence in that the presently proposed method will be useful in the presence of natural samples carrying a more complex background.

5. Conclusions

Complex samples have been analyzed by LC–DAD data which include strongly coeluting analytes, warping of chromatograms in the temporal dimension and presence of uncalibrated interferents. The flexibility of the applied multivariate model (MCR–ALS) allows one to reasonably predict the concentrations of eleven analytes in a set of validation samples. More importantly, in the most challenging analytical scenario, i.e., interfering test samples, five analytes were quantitated within a coeluting cluster of six analyte peaks and three unwanted signals, achieving the second-order advantage which is inherent to second-order LC–DAD information.

Acknowledgements

The following institutions are gratefully acknowledged for financial support: Universidad Nacional de Rosario, CONICET (Consejo Nacional de Investigaciones Científicas y Técnicas, Project PIP 1950) and ANPCyT (Agencia Nacional de Promoción Científica y Tecnológica, Project 25825). R.M.M. thanks CONICET for a postdoctoral fellowship.

References

[1] R. Bro, Crit. Rev. Anal. Chem. 36 (2006) 279–293.
[2] G.M. Escandar, N.K.M. Faber, H.C. Goicoechea, A. Muñoz de La Peña, A.C. Olivieri, R.J. Poppi, Trends Anal. Chem. 26 (2007) 752–765.
[3] M. Daszykowski, B. Walczak, Trends Anal. Chem. 25 (2006) 1081–1096.
[4] A.C. Duarte, S. Capelo, J. Liq. Chromatogr. Rel. Technol. 29 (2006) 1143–1176.
[5] M.C. Ortiz, L. Sarabia, J. Chromatogr. A 1158 (2007) 94–110.
[6] V. Gómez, M.P. Callao, Anal. Chim. Acta 627 (2008) 169–183.
[7] S.A. Bortolato, J.A. Arancibia, G.M. Escandar, Anal. Chem. 80 (2008) 8276–8286.
[8] Y. Zhou, G. Xu, F.F.K. Choi, L.-S. Ding, Q.B. Han, J.Z. Song, C.F. Qiao, Q.S. Zhao, H.-X. Xu, J. Chromatogr. A 1216 (2009) 4847–4858.
[9] S.E.G. Porter, D.R. Stoll, S.C. Rutan, P.W. Carr, J.D. Cohen, Anal. Chem. 78 (2006) 5559–5569.
[10] R. Bro, N. Viereck, M. Toft, H. Toft, P.I. Hansen, S.B. Engelsen, Trends Anal. Chem. 29 (2010) 281–284.
[11] K.S. Booksh, B.R. Kowalski, Anal. Chem. 66 (1994) 782A–791A.
[12] J.W.B. Braga, C.B.G. Bottoli, H.C. Goicoechea, A.C. Olivieri, R.J. Poppi, J. Chromatogr. A 1148 (2007) 200–210.
[13] E. Comas, R.A. Gimeno, J. Ferré, R.M. Marcé, F. Borrull, F.X. Rius, J. Chromatogr. A 1035 (2004) 195–202.
[14] J.A. Arancibia, F. Cañada-Cañada, G.M. Escandar, G.A. Ibañez, A. Espinosa Mansilla, A. Muñoz de la Peña, A.C. Olivieri, J. Chromatogr. A 1219 (2009) 4868–4876.
[15] E. Comas, R.A. Gimeno, J. Ferré, R.M. Marcé, F. Borrull, F.X. Rius, J. Chromatogr. A 988 (2003) 277–284.
[16] A.C. Olivieri, Anal. Chem. 80 (2008) 5713–5720.
[17] R. Tauler, Chemom. Intell. Lab. Syst. 30 (1995) 133–146.
[18] R. Bro, Chemom. Intell. Lab. Syst. 38 (1997) 149–171.

[19] Z.P. Chen, H.L. Wu, J.H. Jiang, Y. Li, R.Q. Yu, Chemom. Intell. Lab. Syst. 52 (2000) 75–86.
[20] H.L. Wu, M. Shibukawa, K. Oguma, J. Chemom. 12 (1998) 1–26.
[21] A.L. Xia, H.L. Wu, D.M. Fang, Y.J. Ding, L.Q. Hu, R.Q. Yu, J. Chemom. 19 (2005) 65–76.
[22] M. Linder, R. Sundberg, Chemom. Intell. Lab. Syst. 42 (1998) 159–178.
[23] M. Linder, R. Sundberg, J. Chemom. 16 (2002) 12–27.
[24] H.C. Goicoechea, A.C. Olivieri, Appl. Spectrosc. 59 (2002) 926–933.
[25] S. Wold, P. Geladi, K. Esbensen, J. Øhman, J. Chemom. 1 (1987) 41–56.
[26] H.A.L. Kiers, J. Chemom. 14 (2000) 105–122.
[27] R. Bro, J. Chemom. 10 (1996) 47–61.
[28] J. Öhman, P. Geladi, S. Wold, J. Chemom. 4 (1990) 79–90.
[29] V.A. Lozano, G.A. Ibañez, A.C. Olivieri, Anal. Chim. Acta 610 (2008) 186–195.
[30] A.C. Olivieri, J. Chemom. 19 (2005) 253–265.
[31] M.J. Culzoni, H.C. Goicoechea, A.P. Pagani, M.A. Cabezón, A.C. Olivieri, Analyst 131 (2006) 718–723.
[32] E. Sanchez, B.R. Kowalski, Anal. Chem. 58 (1986) 496–499.
[33] B.J. Prazen, R.E. Synovec, B.R. Kowalski, Anal. Chem. 70 (1998) 218–225.
[34] K.J. Johnson, B.J. Prazen, D.C. Young, R.E. Synovec, J. Sep. Sci. 27 (2004) 410–416.
[35] S.A. Bortolato, J.A. Arancibia, G.M. Escandar, A.C. Olivieri, Chemom. Intell. Lab. Syst. 101 (2010) 30–37.
[36] R.G. Sadygov, F.M. Maroto, A.F.R. Hühmer, Anal. Chem. 78 (2006) 8207–8217.
[37] N.P.V. Nielsen, J.M. Carstensen, J. Smedsgaard, J. Chromatogr. A 805 (1998) 17–35.
[38] T. Skov, F. van den Berg, G. Tomasi, R. Bro, J. Chemom. 20 (2006) 484–497.
[39] G. Tomasi, F. van den Berg, C. Andersson, J. Chemom. 18 (2004) 231–241.
[40] T. Skov, J.C. Hoggard, R. Bro, R. Synovec, J. Chromatogr. A 1216 (2009) 4020–4029.
[41] Technical Support Center, Office of Ground Water and Drinking Water, United States Environmental Protection Agency, Method 531.2. Measurement of N-methylcarbamoyloximes and N-methylcarbamates in Water by Direct Aqueous Injection HPLC with Postcolumn Derivatization, Cincinatti, Ohio, 2001.
[42] M. Maeder, Anal. Chem. 59 (1987) 527–530.
[43] W. Windig, J. Guilment, Anal. Chem. 63 (1991) 1425–1432.
[44] W. Windig, D.A. Stephenson, Anal. Chem. 64 (1992) 2735–2742.
[45] W. Windig, C.E. Heckler, Chemom. Intell. Lab. Syst. 14 (1992) 195–207.
[46] G.H. Golub, C.F. Van Loan, Matrix Computation, 2nd ed., The Johns Hopkins University Press, Baltimore, 1989.
[47] R. Tauler, A. Smilde, B.R. Kowalski, J. Chemom. 9 (1995) 31–58.
[48] MATLAB 7.0, The Mathworks, Natick, MA, USA, 2007.
[49] J. Jaumot, R. Gargallo, A. de Juan, R. Tauler, Chemom. Intell. Lab. Syst. 76 (2005) 101–110.
[50] J. Saurina, C. Leal, R. Compañó, M. Gramados, M. Dolors Prat, R. Tauler, Anal. Chim. Acta 432 (2001) 241–251.
[51] United States Environmental Protection Agency, Office of Drinking Water Health Advisories, Drinking Water Health Advisory: Pesticides, Lewis Publishers, Chelsea, MI, USA, 1989.
[52] World Health Organization, Guidelines for Drinking Water Quality, vol. 1, World Health Organization, Geneva, Switzerland, 1998.
[53] A.G. González, M.A. Herrador, A.G. Asuero, Talanta 48 (1999) 729–736.